EUROPEAN LABORATORY FOR PARTICLE PHYSICS

CERN-PH-EP-2004-058
CERN-AB-2004-094
11 October 2004

Determination of the bending field integral of the LEP spectrometer dipole

R. Chritin[1], D. Cornuet[1], B. Dehning[1], A. Hidalgo[1], M. Hildreth[1a], W. Kalbreier[1], P. Leclère[1], G. Mugnai[1], J. Palacios[2b], F. Roncarolo[1,3], E. Torrence[1,4c], G. Wilkinson[2]

[1]CERN, European Organisation for Particle Physics, CH-1211 Geneva 23, Switzerland
[2]Department of Physics, University of Oxford, Keble Road, Oxford, OX1 3RH, UK
[3]University of Lausanne, CH-1015 Lausanne, Switzerland
[4]Enrico Fermi Institute and Department of Physics, University of Chicago, Chicago IL 60637, USA
[a]Now at: University of Notre Dame, Notre Dame, Indiana 47405, USA
[b]Now at: Oliver Lodge laboratory, Department of Physics, University of Liverpool, Liverpool, L69 7ZE, UK
[c]Now at: University of Oregon, Department of Physics, Eugene OR 97403, USA

Abstract

The LEP spectrometer performed calibrations of the beam energy in the 2000 LEP run, in order to provide a kinematical constraint for the W boson mass measurement. The beam was deflected in the spectrometer by a steel core dipole, and the bending angle was measured by Beam-Position Monitors on either side of the magnet. The energy determination relies on measuring the change in bending angle when ramping the beam from a reference point at 50 GeV to an energy within the LEP W physics regime, typically 93 GeV. The ratio of integrated bending fields at these settings (approximately $1.18\ \mathrm{Tm}/0.64\ \mathrm{Tm}$) must be known with a precision of a few 10^{-5}.

The paper reports on the field mapping measurements which were conducted to determine the bending integral under a range of excitation currents and coil temperatures. These were made in the laboratory before and after spectrometer operation, using a test-bench equipped with a moving arm, carrying an NMR probe and Hall probes, and in the LEP tunnel itself, with a mapping trolley inside the vacuum chamber. The mapping data are related to local readings supplied by fixed NMR probes in the dipole, and a predictive model developed which shows good consistency for all datasets within the estimated uncertainty, which is 14×10^{-5} for the moving arm, and 3×10^{-5} for the mapping trolley. Measurements are also presented of the field gradient inside the dipole, and of the environmental magnetic fields in the LEP tunnel. When applied to the spectrometer energy calibrations, the bending field model calculates the ratio of integrated fields with an estimated uncertainty of 1.5×10^{-5}.

Accepted by Nucl. Inst. and Meth. A.

1 Introduction to the LEP Spectrometer

The LEP spectrometer was installed close to interaction point 3 of the large electron-positron (LEP) collider in 1999, and took data during 2000. It was designed to measure the beam energy at around 90–100 GeV with a relative precision of $1 - 2 \times 10^{-4}$, a goal which was set by the requirements of the measurement of the W boson mass. Above 60 GeV the transverse polarisation of the beams was very low, and the resonant depolarisation method of energy calibration which was used at LEP 1 [1], was no longer possible.

The principle of the spectrometer is to determine the local beam energy through a measurement of the deflection angle in a dipole magnet of known field. The apparatus consisted of a dipole magnet which was situated between two field-free arms of 10 m in extent. The magnet was an active component of the acceletator lattice, and was ramped in step with the other LEP dipoles. Each arm was instrumented with three Beam-Position Monitors (BPMs), to measure the beam trajectory before and after the magnet.

In order not to place unfeasible demands on the BPM system, the spectrometer was designed and operated to provide a relative energy measurement, in which the measurement at the high energy point of interest is normalised by a reference measurement made in the same fill at a low energy point well determined from resonant depolarisation. The result of the spectrometer measurement at high energy, $E_{\rm b}^{\rm SPECT}$, is then

$$E_{\rm b}^{\rm SPECT} \;=\; E_{\rm b}^{\rm ref}\,\frac{\int B\,{\rm dl}}{\int B\,{\rm dl}^{\,\rm ref}}\,\left(1 \,+\, \frac{\Delta\theta}{\theta_0}\right), \tag{1}$$

where $E_{\rm b}^{\rm ref}$ is the reference energy, typically 50 GeV, $\int B\,{\rm dl}^{\,\rm ref}$ and $\int B\,{\rm dl}$ are the field integrals at the reference point and the high energy setting respectively, and $\Delta\theta$ is the change in bending angle. In practice, as the spectrometer dipole was ramped with the LEP lattice, the bending angle, θ_0, remained approximately constant at a value which was 3.77 mrad, and $\Delta\theta \,<<\, \theta_0$.

The energy calibration with the spectrometer has three sources of systematic error. There is the uncertainty on the knowledge of the ratio $\int B\,{\rm dl}/\int B\,{\rm dl}^{\,\rm ref}$; there are errors associated with the measurement of the change of bend angle; and there is an uncertainty in modelling the synchrotron radiation energy loss and the boosts of the RF system, in order to relate the local energy measured at the spectrometer to the beam energy averaged around the ring. When designing the project it was anticipated that the latter two components would together contribute a relative error of 10^{-4}. Therefore the uncertainty associated with the bending integral ratio should not be more than a few 10^{-5}. This paper reports how this goal was achieved. An account of the other aspects of the spectrometer, including its final performance, and complementary methods of LEP energy calibration for the W boson mass, can be found in [2].

The paper is organised as follows. Section 2 describes the main characteristics of the spectrometer dipole and how it was instrumented during operation. Section 3 explains how the magnetic field integral was mapped in the laboratory, and how a model was constructed to predict the field integral from local field readings. Results are also given on other relevant aspects of the magnetic field characteristics. Section 4 describes a complementary mapping technique, which was used to cross-check the laboratory results after the installation of the dipole in the LEP tunnel. Section 5 briefly discusses sources of magnetic field in the tunnel external to the dipole. Section 6 presents the results of the field integral model applied to the spectrometer energy calibration measurements, and section 7 gives the conclusions of the work.

2 The Spectrometer Dipole

The spectrometer dipole was a C-shaped steel core magnet, similar in design to those used in the LEP injection region, which was manufactured by industry [3] and assembled at CERN. It measured 5.75 m in length (z-axis) and had an aperture of 25.4 cm transverse (x-axis) by 10.0 cm vertical (y-axis). The yoke was constructed from 1.5 mm thick laminations made of low carbon steel, stacked between two 30 mm thick massive end plates. Two 24 mm diameter steel rods running in the longitudinal direction held the end plates together and provided stabilization against twist. The robustness was further enhanced by mounting the yoke on a steel support girder. The design ensured that any mechanical deformations were smaller than 0.15 mm. Two racetrack shape coils, each consisting of 18 windings, surrounded the upper and lower magnet poles. The total weight of the magnet and girder was 10.3 Tonnes. A photograph of the dipole after LEP dismantling can be seen in in figure 1, with the main features indicated.

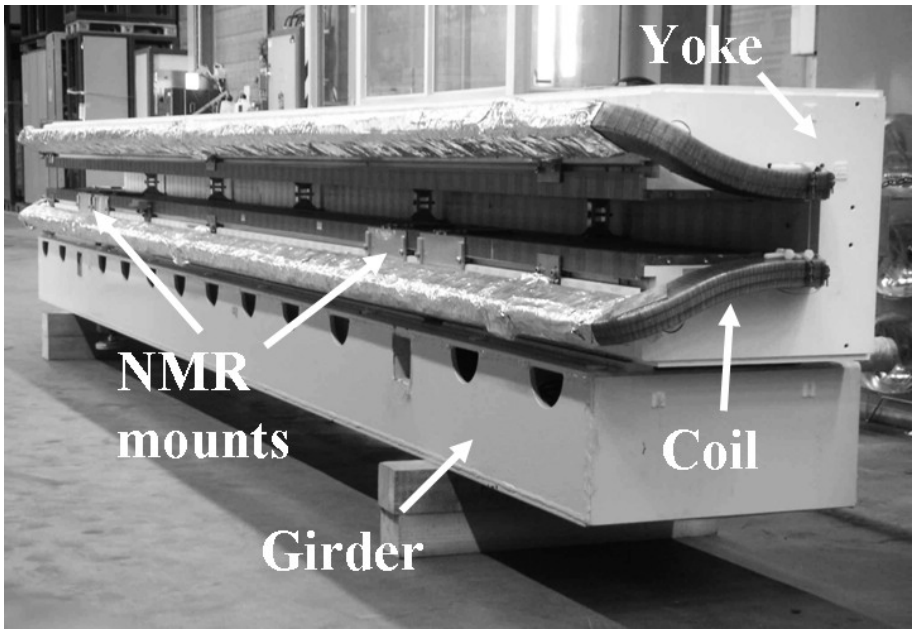

Figure 1: Photograph of the spectrometer dipole after LEP dismantling.

When LEP was operating with a nominal beam energy of 100 GeV, the spectrometer dipole was required to provide an integrated bending field of 1.27 Tm, corresponding to a local field of approximately 0.22 T in the core region, when powered by an excitation current of 480 A. In this paper all magnet settings will be expressed in terms of equivalent beam energy. By providing a field strength of approximately double that of a conventional concrete core LEP arc dipole, over a similar distance, the spectrometer dipole was able to replace two such magnets in the LEP lattice, and make space available for the BPM stations and associated instrumentation.

In order to ensure the optimal thermal stability, the temperature of the coil was regulated with a water cooling system independent of the global circuit used for the other LEP dipoles. One feedback loop maintained a constant input water temperature, and a second feedback loop controlled the flow rate in order to minimise any variation detected in the output water temperature. This system dissipated the power induced by Joule heating in the coils and incident synchrotron radiation, and restricted the temperature rise in ramping between the reference

point and high energy to $3-4^{\circ}$ C. These residual temperature changes were monitored by 34 PT100 temperature probes installed in a variety of locations.

The dipole was equipped with two pairs of fixed NMR probes to provide continuous local reference readings of the B-field. Each pair consisted of a 'type-1' and 'type-2' probe (Metrolab 1062-1 and 1062-2 [4]), both placed on the lower pole piece of the dipole. The type-1 probes were sensitive to fields corresponding to low energies, of 22 GeV and above, but saturated at settings beyond 60 GeV. The type-2 probes were optimised for higher fields, and had an initial locking threshold of 40 GeV. The specification of the field measurement accuracy was $< 5\,\mathrm{ppm}$ absolute and $0.1\,\mathrm{ppm}$ relative. The active area of the probe heads was approximately $5 \times 5\,\mathrm{mm}^2$.

During operation the probes sustained damage from synchrotron radiation, which degraded their read-out efficiency and led to a rise in the locking threshold. In order to have reliable data over the full range of field settings it was therefore necessary to replace the probes several times during the year. When installing NMR probes in the standard LEP dipoles, steel field plates were used to enhance the local field uniformity. In the spectrometer, however, in order to minimise the additional magnetic material outside the dipole yoke itself, no such field plates were inserted. For this reason it was particularly important to choose locations for the probes where the local field was as uniform as possible. Figure 2 shows a scan made of the variation in B field with longitudinal and transverse position around a candidate probe location. Regions of high field gradient can be seen, associated with the laminations of the dipole core, as well as regions where the field is more stable. The four probe locations were defined by the requirement that the relative B field gradient be less than 10^{-5} /mm in all directions. Precision mounts ensured that the probes remained fixed in these locations to within 0.5 mm throughout the mapping campaigns, and all spectrometer operation.

3 Moving Arm Mapping Campaigns

In the Winter of 1998-9, prior to the spectrometer installation in LEP, a test-bench was set up to perform field mapping of the dipole, employing an NMR probe and two Hall probes mounted on a moving arm. The field maps made with this apparatus form the dataset of the *pre-installation* mapping campaign. After the dismantling of LEP, a further programme of mapping was performed during 2001-02. This *post-LEP* campaign used the same test-bench as previously, but took place in a different laboratory with some improvements to the apparatus.

Integrated field maps from both campaigns are related to local field readings provided by fixed reference probes, in order to produce a bending field model which can be used during spectrometer experiments.

3.1 Apparatus and Data Taking

The mapping apparatus is shown in figure 3. A high-thermal inertia marble block of dimensions $6.2 \times 0.6 \times 0.6$ m, and of mass 6000 kg was placed parallel to the dipole. A mapping carriage, driven by a motor, ran along cog-rails, which were mounted longitudinally on the block. The location of the carriage along the rails was controlled to a relative accuracy of 5×10^{-6} through reference to a steel linear encoder (Heidenhain, LIDA 105 C [5]), which was attached to either end of the block.

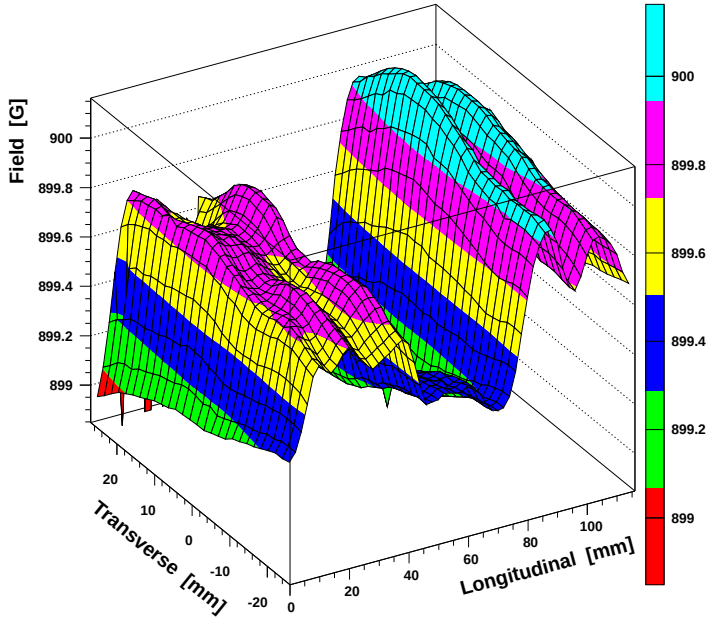

Figure 2: Variation of the B-field with position in the spectrometer dipole as measured in a region of 100 mm (longitudinal) by 50 mm (transverse) at 41 GeV. (The origin is arbitrary). The plateau region at low longitudinal values is a suitable location for an NMR reference probe.

The mapping carriage held two transverse rods which supported the measuring arm. In the pre-installation campaign these rods were made from stainless steel. For the second campaign they were replaced with aluminium alloy in order to minimise the residual magnetic material in the apparatus. When the measuring arm was centred on the magnet-axis, the separation between the arm and the marble block was 65 cm. This distance could be changed with a motor which acted upon one of the support rods. The extension of the arm was monitored with a linear encoder.

The measuring arm was a low-mass rigid cage of 2 m in length, formed by four carbon-fiber tubes. It was equipped with an NMR probe to measure the field profile of the core region, and two Hall probes to map out the end-fields, where, due to the steep field gradient, the NMR probe no longer locked. The sensitive head of the NMR probe was positioned in the centre of the arm. The longitudinal axis of the probe body was parallel to the arm in the pre-installation campaign, and perpendicular to the arm in the post-LEP campaign. The Hall probes were situated 85 cm to the left (Hall L) and the right (Hall R) of the arm centre. Brass screws were used everywhere to avoid introducing magnetic material into the dipole aperture. The NMR probe was of the 'type-2' type, identical to those used to provide the fixed local measurements. The Hall probes were regulated at a temperature of $40^\circ \pm 0.02^\circ\,\mathrm{C}$, and were of a design which had a sensitive area of $1.6 \times 1.6\,\mathrm{mm}^2$ in the pre-installation campaign and $0.35 \times 0.35\,\mathrm{mm}^2$ in the post-LEP campaign (Siemens SBV579 and KSY44 respectively [6]).

In preparing the dipole for each mapping session, a procedure was followed which was very similar to that used during LEP operation:

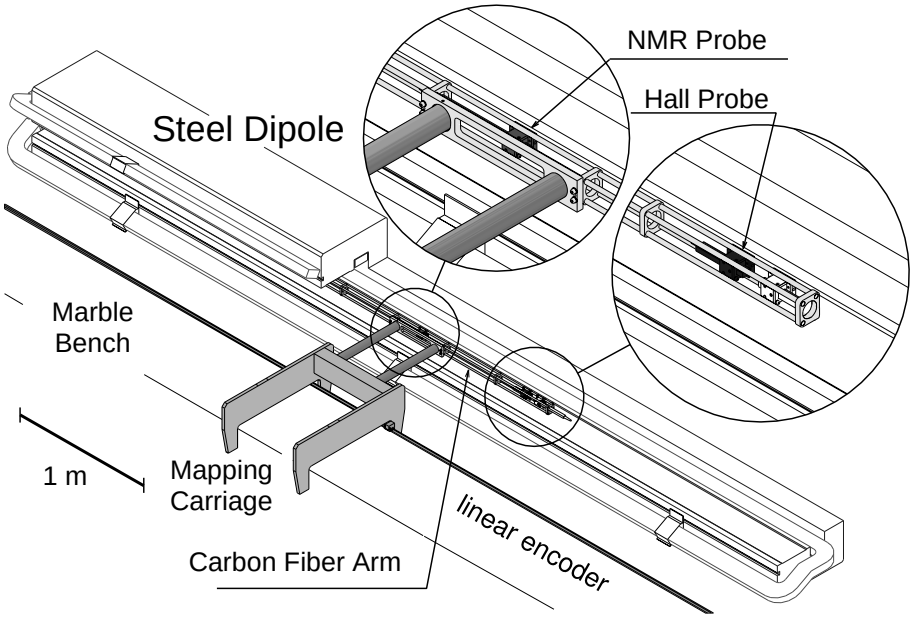

Figure 3: The magnetic mapping test-bench, showing inset the components of the moving arm.

- **Degaussing Cycle** The current was cycled from 5 A to 500 A and back to 5 A at a ramp speed of 50 A/s. The operation was repeated five times, with a 5 s pause at the top and bottom of each cycle. This cycling was performed to suppress any parasitic remanent field and to ensure that the dipole followed the same hysterisis curve during the ramp.

- **Ramp** The current was ramped to its nominal setting at a rate of 2.3 A/s, with a 5 minute pause at an intermediate setting of 22 GeV, corresponding to the energy at which injection took place during LEP running.

- **Bending Modulation** The current was raised by 0.03%, and then dropped back to its nominal setting, seven times, at a ramp speed of 2.3 A/s, with a 2 s pause at the top and bottom of each cycle. This operation was performed in order to condition the magnet and improve the field stability, as discussed in [1].

One or more maps were then taken at the desired setting. Each map consisted of roughly 550 individual arm readings separated by 1 cm, which took approximately half an hour to accumulate. After mapping was complete, the current was either lowered to zero, or raised to a higher setting where, after another sequence of bending modulation, new mapping would begin.

The pre-installation campaign accumulated around 150 maps at energies between 41 GeV and 103 GeV. A small number of additional maps were made to explore temperature effects and the vertical and transverse uniformity of the field. Roughly twice as many maps were made during the post-LEP campaign.

The field profile at 100 GeV is shown in figure 4 (a), indicating the relative extent of the core region measured by the travelling NMR, and the end fields measured by the Hall probes. In both the mapping laboratories and in the LEP tunnel these end fields were truncated 0.5 m away from the dipole with magnetic shields, These shields were made of three concentric layers of 0.2 mm thick mu-metal, 50 cm in length, wrapped around the vacuum chamber. Measurements made with a fluxgate magnetometer showed the residual absolute field inside the mu-metal to

be less than 50 mG. The end fields make up 8.3% of the total field integral. This contribution has a very weak energy dependence of $2 \times 10^{-6}/\,\mathrm{GeV}$.

Figure 4 (a) also shows a zoom into the core region for a single map, to illustrate the uniformity of the field. The small fluctuations that exist are tracked by both the NMR and the Hall probes, indicating that the relative precision of the Hall probes is better than 10^{-4}. Small displacements are seen, however, between the three sets of measurements. These displacements vary from map to map and are attributed to drifts in the absolute calibration scale of the Hall probes. In the analysis map-by-map correction factors are applied to each set of Hall probe readings to compensate for these drifts. In addition, offsets are applied to each Hall probe to correct for small non-zero readings observed deep within the mu-metal shields, which are also evidence of imperfect calibration.

The structure visible in the core region zoom is seen in all maps, and at all magnet settings. Figure 4 (b) shows the travelling NMR data for both a 100 GeV map and a map made at 41 GeV, as well as the ratio between these measurements. The relative shape of the field, away from the magnet ends, is reproduced to better than 10^{-4}.

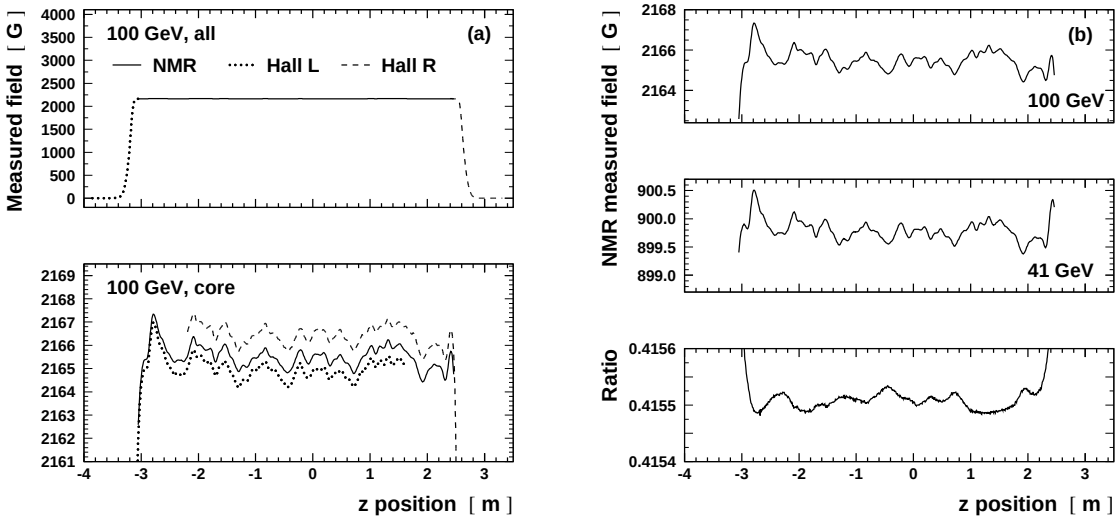

Figure 4: The longitudinal profile of the spectrometer dipole field as measured with the moving arm apparatus. (The arbitrary origin is defined by the mapping test-bench.) (a) shows the entire profile at 100 GeV, and a zoom into the core region. The Hall probe data are displayed with the nominal calibration coefficients, prior to correction. (b) shows the NMR data for a map at 100 GeV and a map at 41 GeV, and the ratio between the two.

For each map it is necessary to define a local field value, B_{loc} for each of the fixed NMR probes, in order to provided reference values to be used in the bending field model. The duration of an individual map is sufficiently short that this can be done by merely calculating the mean of the readings from each fixed probe. Prior to calculating this mean for the pre-installation maps, however, it is necessary to exclude those data when the moving arm is in the vicinity of the fixed probe of interest. This is because magnetic material in the arm led to distortions in the local field. These distortions can be seen as one large spike and several smaller bumps in figure 5. The spike is associated with a small variable ferromagnetic capacitor in the body of the

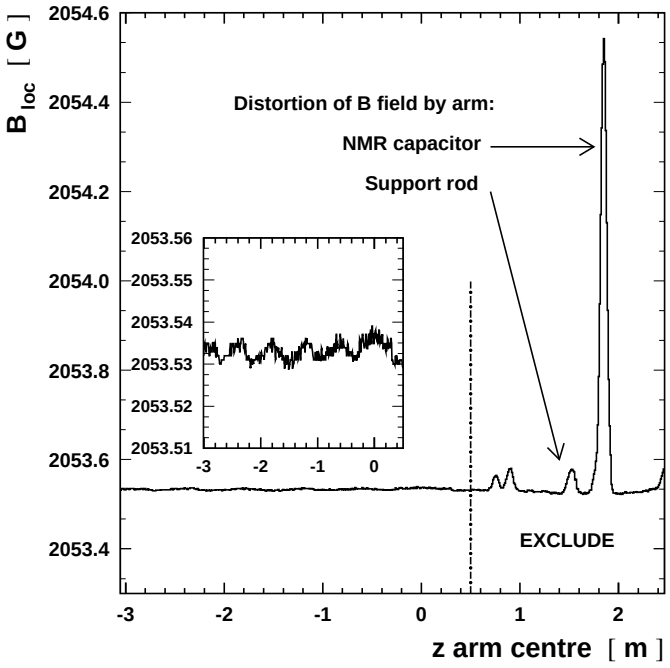

Figure 5: A local field reading from the pre-installation campaign, measured by one of the fixed NMR probes located close to $z = 2$ m, as the position of the scanning arm changes. Distortions of the local field reading are observed when the centre of the moving arm is close by. The inset shows a zoom of the remaining readings when the distorted region is excluded.

moving NMR probe, and the bumps with the stainless steel arms which supported the arm. The inset region in figure 5 shows the data from which $B_{\rm loc}$ is calculated. The probe readings are stable to better than 10^{-6}. The distortions were suppressed entirely in the post-LEP campaign, through using aluminium alloy support arms and through rotating the moving NMR probe body in the horizontal plane, so that the capacitor no longer passed over the head of the fixed probe.

3.2 Results on the Bending Field Integral Measurements

For each map the NMR probe and corrected Hall probe data are used to calculate the field integral. In this calculation the trapezium method is used to approximate the step-by-step readings to the true integral.

The spread in measured integrals at several equivalent beam energy settings are given in the 'Raw RMS' columns of table 1, for both mapping campaigns. For the sample of maps analysed here, the magnet coil temperature is approximately constant at each analysis point (RMS over maps $\leq 0.1^\circ$ C). Prior to calculating these spreads, a linear scaling has been applied to correct for any small measured differences in excitation current at each setting. It can be seen that the field integral is measured with a map-to-map mean scatter of approximately 2×10^{-5} Tm in both campaigns. (The spreads of the residuals to the bending field model, which are given in the 'Resids RMS' column, are discussed in section 3.3.)

There are several possible sources of systematic bias on the measurement of the field integral, all of which arise because of the significant gradient of the end field. These are estimated

E_b^{equiv} [GeV]	Pre-installation campaign			Post-LEP campaign		
	Number of maps	Raw RMS [Tm] $\times 10^{-5}$	Resids RMS [Tm] $\times 10^{-5}$	Number of maps	Raw RMS [Tm] $\times 10^{-5}$	Resids RMS [Tm] $\times 10^{-5}$
41	12	0.5	0.5	69	6.3	0.4
44	41	4.4	0.7	2	/	/
50	16	0.4	0.4	28	0.6	0.2
55	3	/	/	19	0.2	0.1
60	19	3.9	0.6	20	0.6	0.4
70	11	0.5	0.7	6	0.4	0.5
80	30	0.5	0.5	29	1.0	0.3
90	14	0.5	0.4	56	1.5	0.3
100	6	0.5	0.7	106	2.4	0.7
Mean	/	2.0	0.6	/	2.5	0.4

Table 1: Summary of scatter in measured field integrals ('Raw RMS') and fit residuals ('Resids RMS') for various nominal energy points in the pre-installation and post-LEP mapping campaigns. In both cases the model used to evaluate the fit residuals derives from a fit to the post-LEP data. The 100 GeV point corresponds to a bending field integral of 1.27 Tm.

by fitting a polynomial to the profile of the end field, and using this form in a simulation to calculate the error induced on the total field from each source. They are as follows:

- The trapezium sum, performed to approximate the field integral, underestimates the true value by a relative 2×10^{-5}.
- The finite sampling size of the Hall plate means that in a non-linear field, the measured field value is systematically shifted from the true field value at the centre of the plate [7]. Calculations show the effect leads to a relative shift in the total field integral of $< 0.5 \times 10^{-5}$ in the first campaign, and is entirely negligible for the post-LEP measurements, where smaller probes were used.
- There is an uncertainty of $150\ \mu\mathrm{m}$ on the location of the semiconductor Hall plate with respect to the probe casing. This introduces a systematic error on the single end field integral of 6.6×10^{-4}. The uncertainty is uncorrelated between probes, and thus the combined error from both arms on the total field integral is 12×10^{-5}. An additional uncertainty of 8×10^{-5} comes about from an estimated $100\ \mu\mathrm{m}$ alignment error on the mounting of each Hall probe on the mapping arm.

The total uncertainty on the field integral measurements made with the travelling arm is therefore 14×10^{-5}. All of these biases are correlated between measurements, and largely cancel when considering the ratio of bending field integrals at different energies.

3.3 The Bending Field Model

It is necessary to be able to model the thermal dependence of the bending field in order to be able to know the effect of temperature variations during spectrometer measurements. Any change

of field integral with temperature in the core region is in principle tracked by corresponding changes in the readings of the fixed NMR probes, but the end fields can evolve in a different manner. In order to accommodate this difference in behaviour the local field from each fixed NMR, $B_{\rm loc}$, is corrected to

$$B_{\rm loc}^{\rm cor} = \left[1 + C_T^{\rm eff} \left(T - T_{\rm ref} \right) \right] B_{\rm loc}.$$

Here T is the temperature of the coil and $T_{\rm ref}$ is a reference temperature chosen to be $34^{\circ}{\rm C}$, the mean coil temperature for the majority of the maps. $C_T^{\rm eff}$ is an effective temperature coefficient, which depends on the temperature coefficient of the core field, $C_T^{\rm core}$, and the temperature coefficient of the end field, $C_T^{\rm end}$, in the following manner:

$$C_T^{\rm eff} = f_{\rm end} \left(C_T^{\rm end} - C_T^{\rm core} \right),$$

where $f_{\rm end} = 0.083$ is the fraction of the integrated bending field outside the core region. Each temperature coefficient is determined by comparing maps at coil temperatures of $T_{\rm ref}$ with those taken at temperatures up to 10° C higher. The following values are obtained: $C_T^{\rm core} = -0.9 \pm 0.5 \times 10^{-5} / ^{\circ}$ C, $C_T^{\rm end} = 7.8 \pm 0.8 \times 10^{-5} / ^{\circ}$ C, and hence $C_T^{\rm eff} = 7.3 \pm 0.7 \times 10^{-6} / ^{\circ}$ C. The negative sign of the core field coefficient can be attributed to the widening of the dipole aperture with temperature, whilst the positive sign of the end field coefficient is associated with the expansion of the coils as the magnet heats. No evidence is seen of the coefficients having a significant dependence on the thermal history of the magnet, in contrast to what was observed when studying the standard LEP concrete core dipoles [1].

In fitting the bending field model, the maps are first divided into bins of equivalent beam energy. For each probe, a separate two parameter fit is made between the field integral and $B_{\rm loc}^{\rm cor}$. The fitted coefficients then allow the field integral to be predicted from a given local NMR reading. These predictions, averaged over all available probes, define the output of the bending field model. The *pre-installation model* refers to the model fitted to the data of the first campaign; the *post-LEP model* refers to the model fitted to the data accumulated after LEP dismantling.

The relative fit residuals of maps from the pre-installation campaign are shown in figure 6 (a), divided into data taken at coil temperatures close to $T_{\rm ref}$ ('Standard maps') and those taken at higher temperature ('Warm maps'). Separate results are shown for the pre-installation model fitted with and without a temperature correction applied to the fixed probe readings. With the correction included, the residuals exhibit no futher temperature dependence.

Fit residuals have been calculated for the dataset of table 1, using the post-LEP model. The RMS scatters of these residuals are shown in the column marked 'Resids RMS'. It can be seen that the spreads are similar for both datasets, and have a typical value of 0.5×10^{-5} Tm, which is significantly smaller than the scatter of the raw data.

In figure 6 (b) are shown the relative fit residuals of the post-LEP model evaluated on all travelling arm data for the pre-installation ('Arm') and post-LEP ('Arm, new Hall probes') campaigns. (The points marked 'Trolley' are discussed in section 4). For both sets of maps, the plotted points show very little dependence on energy, indicating that any non-linearities in the relationship between the local field and the measured field integral are small. However, an offset of approximately 8×10^{-5} is seen between the two datasets. This shift arises from differences in the end field contributions to the residuals, and can be attributed to the change in

Hall probes between the two campaigns. As discussed in section 3.2, the uncertainty in Hall plate position within a probe introduces a significant uncertainty on the measurement of the end field, and hence $\sim 10^{-4}$ shifts are to be expected when comparing the results of different probes. This hypothesis was verified by re-equipping the travelling arm with the older probes and taking additional maps during the post-LEP campaign. The relative residuals for these data ('Arm, old Hall probes') are included in figure 6 (b) and agree very well with the pre-installation results, also suggesting that the reproducibility of the probe alignment on the arm is better than $100\ \mu$m.

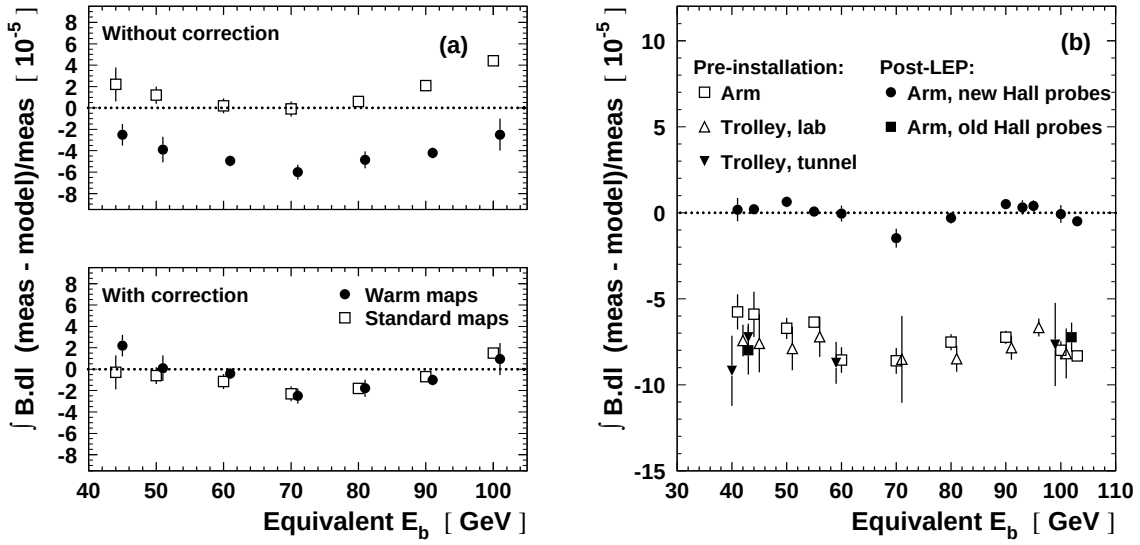

Figure 6: Relative residuals of the bending field model at different magnet settings, expressed as equivalent beam energies. (a) shows the results for the pre-installation travelling arm data, evaluated with a model fitted to these data, with and without a temperature correction. (b) shows the results for all maps using the post-LEP model, including temperature correction. The error bars represent the RMS over the maps in each energy bin.

3.4 Field Gradient Measurements

The standard maps were made with the arm travelling along the axis of the dipole. The LEP beam, however, describes an arc with a sagitta of around 6 mm. Therefore it was important to probe the transverse homogeneity of the field integral to verify that the mapping data were valid for LEP operation.

Maps were made with the arm positioned at different horizontal displacements from the dipole axis. In total, a range of 20 mm was spanned, at a variety of excitation currents. These maps showed that a transverse relative field gradient existed in the core region of approximately 5×10^{-6} /mm. The gradient in the end field region, however, was found to be of the opposite sign and an order of magnitude larger. The integrated bending field, therefore, is very stable under transverse displacement, varying by less than a relative 5×10^{-6} over the region probed by the beam. These observations are consistent with the predictions of field calculations [8]. The effect is sufficiently small that it can be neglected in the bending field model.

Maps were also performed with the NMR displaced vertically in order to probe the variation of the field in this direction. A relative field gradient of $3 \pm 2 \times 10^{-6}$ /mm was measured.

The spectrometer was aligned in the tunnel so that the beam passed within 1 mm of the magnetic axis of the dipole. In energy measurements the beam was steered such that the position at the high energy and low energy points was identical to within a few $100\ \mu\mathrm{m}$. Therefore no significant uncertainty enters into the knowledge of the ratio of field integrals from this source.

4 Trolley Mapping

A second field-mapping technique was developed in order to verify that the results of the moving arm test-bench remained valid when the magnet was installed in the LEP tunnel, with the vacuum chamber in place. This method consisted of a trolley carrying magnetic measuring equipment which could perform maps inside the vacuum chamber itself. Maps were made with this method in 1999, both during the pre-installation moving arm laboratory and in the LEP tunnel. In both cases a segment of vacuum chamber was inserted into the dipole gap.

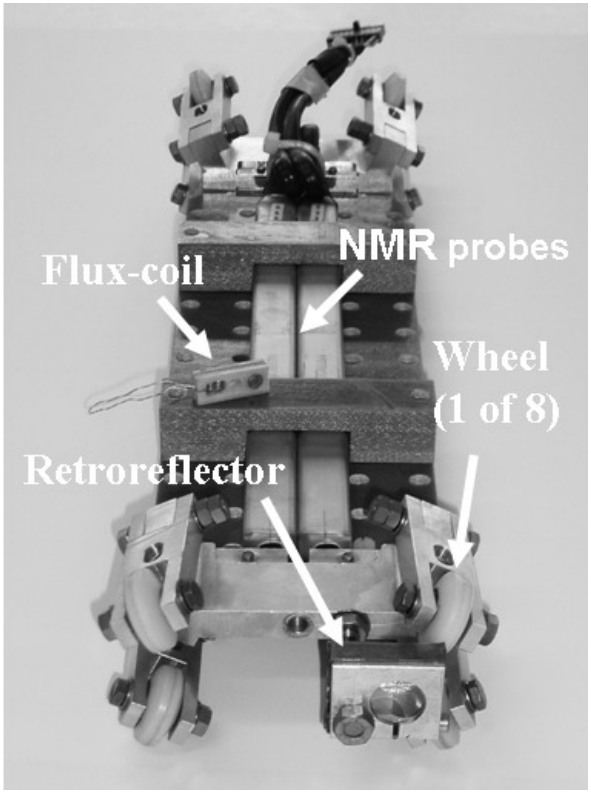

Figure 7: Front-view photograph of the mapping trolley, with the main features indicated. (Note that during operation the flux-coil is mounted under the NMR probes.) The trolley is 41 cm long and 9 cm wide.

A photograph of the mapping trolley is shown in figure 7. It was constructed out of non-magnetic materials, with the chassis being made out of aluminium and fiberglass. The Teflon wheels provided eight points of contact with the elliptical walls of the vacuum chamber, and were inclined at an angle chosen to give the trolley maximum stability against rotations. Bronze-

beryllium springs inserted in the upper wheel supports ensured firm contact with the vacuum chamber walls.

The trolley carried two type-2 NMR probes, separated by 1.5 cm transversally, and a flux-coil, located directly underneath the probe heads, in order to measure the end-field regions. The flux-coil consisted of 1000 turns wrapped around a rectangular frame of 2.5 (transverse) $\times\, 1.0$ (longitudinal) cm^2. The voltage induced in the coil as the trolley moved was fed into a digital integrator. Data accumulated in 5 s periods before and after the trolley movements allowed amplifier drifts to be corrected for. The exact area of the coil was determined by comparing the time integrated induced voltage with the change in flux-density as measured by the NMR probes, while the trolley was held stationary and the magnet was ramped between two settings. This calibration was found to be stable with time.

A toothed Kevlar belt was clamped to the front and the back of the trolley. The belt was looped around two pulleys mounted at either end of the vacuum chamber segment. One of these pulleys was driven by a stepping motor. The signals and power leads for the NMRs and flux-coil were carried in a flat-cable which was independently supported so as not to exert tension or torque on the trolley. On the back of the trolley was mounted a retroreflector, which allowed an interferometer to measure the longitudinal position of the trolley with a relative precision of 1×10^{-6}.

The magnet was prepared for mapping following the same procedure described in section 3.1. In each map the step-size of the trolley movements was set to 2 cm in the core region and 1 cm for the end-fields. Each map took about 30 minutes to perform. In the laboratory, maps were made at the same settings that were used for the pre-installation moving arm campaign. In the tunnel, time limitations restricted the choice to a subset of these energies.

The relative residuals of the trolley data to the post-LEP model are included in figure 6 (b). The laboratory and tunnel residuals are consistent with each other, indicating that the installation in the tunnel did not affect the behaviour of the magnet. There is no evidence of any significant non-linearity.

The systematic error on the trolley measurements is dominated by the uncertainties associated with the knowledge of the end-fields. A relative 2×10^{-5} error on the total integral arises from the intrinsic precision of the flux-coil. This is assigned by comparing the flux-coil and NMR estimates of the core-region field integral. Respective contributions of 2×10^{-5} and 1×10^{-5} come from the trapezium sum approximation, and the bias related to the finite sampling size of the coil. The uncertainty in the exact position of the flux-coil does not introduce any significant error in the total field integral, since any bias in the measurement of the end-field integrals is of opposite sign, and similar magnitude, at the two ends of the dipole. The total relative error on the total bending field integral is therefore 3×10^{-5}, which is less than the uncertainty on the moving arm measurements. The good agreement between the trolley residuals and the pre-installation moving arm results imply that the Hall plates were closest to their nominal positions in the first campaign.

Comparison of the data from the two side-by-side probes on the trolley confirmed the measurements of the transverse field gradient in the core region made with the moving arm. Further information on the trolley mapping may be found in [9].

5 Environmental Magnetic Fields

After the installation of the spectrometer, measurements were made of the environmental magnetic field in the LEP tunnel, in the supposed field-free region of the BPM arms, either side of the dipole magnet. These measurements were performed with fluxgate magnetometers [10] Data were taken at a variety of machine settings. Examples are shown in figure 8, which give the field readings in the vertical direction as a function of distance from the dipole centre, for settings corresponding to 0 GeV, 50 GeV and 93 GeV. When there is no power, a downwards field is observed, coming from the earth itself. Two local upwards spikes are seen, originating from permanent magnets situated in vacuum pumps. When the machine is on, an additional field contribution arises from the magnet cables. This component is in the opposite sense to the earth field and varies in size with the LEP energy.

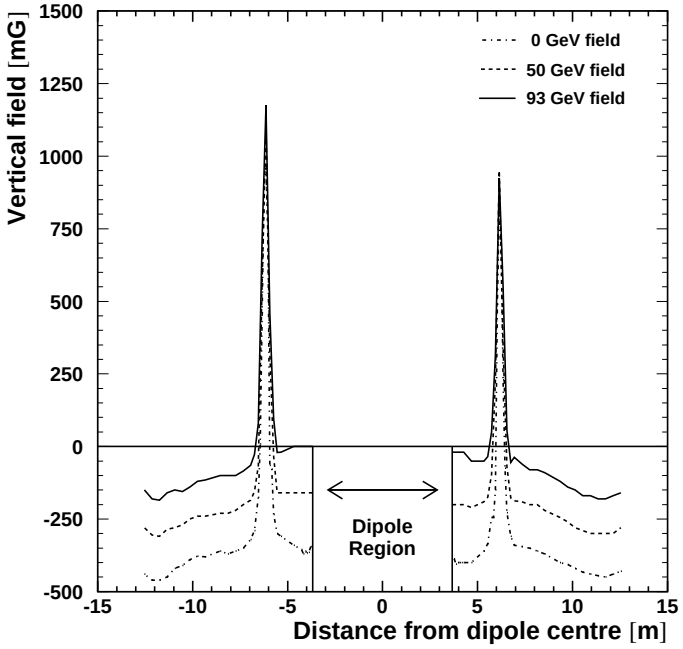

Figure 8: Environmental magnetic field readings in the vertical direction as a function of longitudinal distance along the spectrometer. (The data were taken with LEP configured with the so-called ‘polarisation optics’). The large spikes are caused by permanent magnets situated in vacuum pumps.

In the spectrometer energy determination, the environmental field was taken into account when analysing the beam trajectories through the BPM arms. This procedure is discussed in [2].

Stationary fluxgates monitored the environmental field in selected locations throughout the 2000 run. Good stability with time was observed.

6 Application to the 2000 Spectrometer Measurements

The calibration of the LEP beam energy performed with the spectrometer in 2000, as detailed in [2], derives from 15 individual experiments. In each experiment data were taken at a reference low energy setting of 50 GeV, and at a high energy point, which varied between 90 and 97 GeV. The local energy at the spectrometer is determined with expression 1, taking as input data the measured change of bending angle, and the ratio of field integrals, $\int B\,\mathrm{dl}/\int B\,\mathrm{dl}^{\mathrm{ref}}$. For the central value of the spectrometer energy analysis presented in [2], the post-LEP bending field model is used [1]. In this calculation, the very small values of the model residuals to the post-LEP data, observed in figure 6 (b), are applied as corrections.

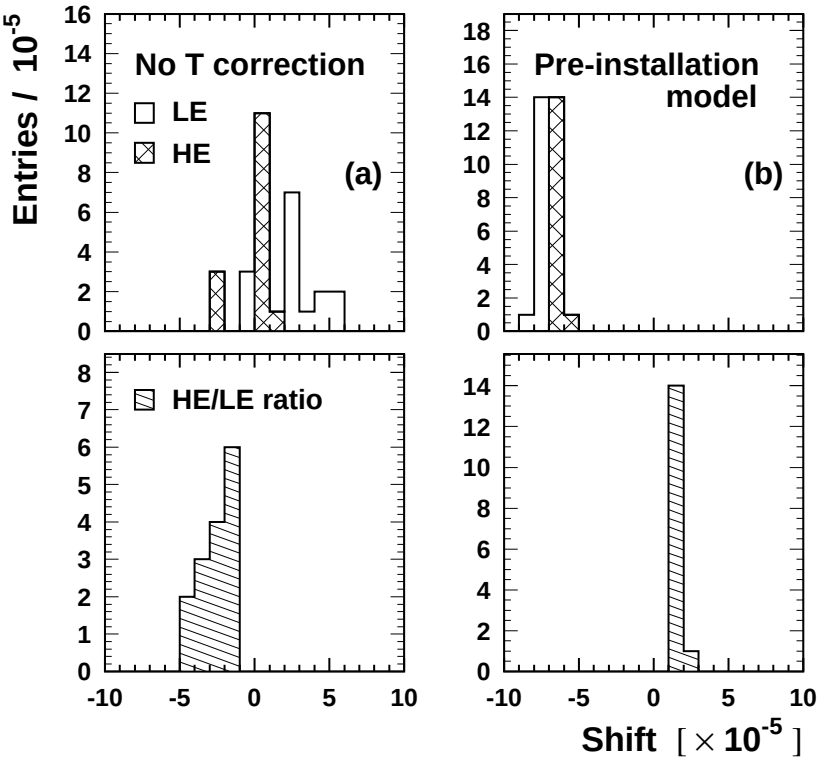

Figure 9: Relative shifts seen in the calculation of the dipole field integral, and the ratio of field integrals, for the 2000 spectrometer experiments. In the top plots separate entries are shown for the high energy (HE) and low energy (LE) points of the 15 energy calibration measurements. In the lower plots the shifts in the ratios between high and low energy integrals are shown. All shifts are expressed with respect to the post-LEP model, including temperature correction. (a) and (c) show the effect of excluding the temperature correction entirely. (b) and (d) show the effect of using the pre-installation model.

[1] Although the good agreement between the pre-installation travelling arm and trolley data suggest that there is a small bias in the end-field measurements of the post-LEP campaign, the latter dataset is preferred for fixing the central value of the $\int B\,\mathrm{dl}/\int B\,\mathrm{dl}^{\mathrm{ref}}$ ratio, as it has significantly more maps at 50 GeV and 90–100 GeV.

Alternative bending field models have been used to assess the systematic uncertainty on the energy calibration from the knowledge of $\int B\,\mathrm{dl}/\int B\,\mathrm{dl}^{\mathrm{ref}}$. Figure 9 shows the shift in results observed when two of these models are introduced. Results are shown separately for the high and low energy points, and for the ratio of the field integrals between the two settings. Plots 9 (a) and (c) display how the results change when the temperature correction is removed. A more significant effect is seen at low energy than high energy because the mean coil temperature of the high energy setting is closer to the reference value used to fit the model. The shift on the ratio is -2.6×10^{-5}. Since the uncertainty on the understanding of the temperature dependence is 10%, the resulting error on the energy measurement, when using the complete model, is negligible.

Plots 9 (b) and (d) show the offsets observed when the pre-installation model is applied. The calculated bending fields shift by up to -8×10^{-5}, whereas the ratio moves by only 1.5×10^{-5}. This shift is taken as the systematic uncertainty on the knowledge of the ratio $\int B\,\mathrm{dl}/\int B\,\mathrm{dl}^{\mathrm{ref}}$, as the variations observed when switching to all other models are significantly smaller.

7 Conclusions

The field characteristics of the LEP spectrometer dipole magnet have been investigated in the laboratory with a moving arm test-bench. Two campaigns, conducted before installation and after dismantling, have allowed the stability of the magnet behaviour to be assessed. Data obtained through a complementary method, involving a mapping trolley inside the vacuum chamber, provide a constraint on the dipole field after installation. All results are consistent within the assigned errors. The most precise measurements of the field integral come from the mapping trolley, and have a relative uncertainty of 3×10^{-5}.

A model has been developed which enables the total field integral to be calculated as a function of local NMR probe readings, and the temperature of the magnet coil. For all datasets, this model exhibits good linearity over the energy range relevant for the energy measurement. The RMS scatters on the residuals of the model predictions to the mapping data are around 5×10^{-6}, indicating that the magnet behaviour is well understood and very reproducible.

The systematic uncertainty on the ratio of high energy to reference field integrals in the spectrometer measurements is assigned by considering the change in result when different variants of model are used to calculate the field integral. The largest shift observed is 1.5×10^{-5}. An identical relative error results on the energy determination. Uncertainties related to the temperature modelling and the transverse and vertical field gradients introduce negligible additional uncertainty to this ratio. This systematic error is small compared to the other sources of uncertainty in the spectrometer analysis.

Acknowledgements

We are grateful to G. De Rijk, I. Ruehl, M. Sassowsky and W. Weterings, whose expertise was invaluable in the design, construction and operation of the spectrometer dipole.

We also acknowledge the support of the Particle Physics and Astronomy Research Council, UK, and the National Science Foundation, USA.

References

[1] R. Assmann *et al.* (LEP Energy Working Group), Eur. Phys. J. **C6** (1999) 187.

[2] R. Assmann *et al.* (LEP Energy Working Group), *Calibration of centre-of-mass energies at LEP 2 for a precise measurement of the W boson mass*, CERN-PH-EP-2004-032, CERN-AB-2004-030 OP, submitted to Eur. Phys. J. C.

[3] Tesla Engineering Ltd, Water Lane, Storrington, West Sussex, RH20 3EA, UK. http://www.tesla.co.uk

[4] Metrolab Instruments S.A., Geneva, Switzerland. http://www.metrolab.com

[5] Heidenhain Corporation. http://www.heidenhain.com

[6] The Hall probe characteristics and performances are evaluated in:
P. Leclère, *Test de stabilité de différentes sondes de Hall*, CERN-SL-99-060 MS.

[7] B. Berkes, *Influence of magnetic gradient fields on the Hall effect*, IMMW 2001, Grenoble, France, *http://www.esrf.fr/conferences/proceedings/IMMW12/*.

[8] M. Sassowsky, *Magnetic field calculations for the LEP spectrometer project*, CERN-SL-99-011 MS.

[9] F. Roncarolo, *The LEP Spectrometer Project: High Accuracy Magnetic Field Mapping of the Spectrometer Magnet*, Tesi di Laurea in Ing. Nucleare (2000), Politecino di Milano

[10] Applied Physics Systems, 1245 Space Park Way, Mountain View, CA 94043 USA. http://www.appliedphysics.com